# Chapter 5

# Facile and sensitive colorimetric assay of choline based on AuNps@$WS_2$-QDs as a peroxidase mimetic

## 5.1 Introduction

Choline is an essential precursor for production of acetylcholine (neurotransmitter), due to the presence of quaternary amine (Trimethyl-β-hydroxyl-ethylammonium) which is crucial nutrient for humans[Blusztajn, 1998]. The deficiency of choline in human, creates various health problems like hemorrhagic kidney necrosis, liver disease, atherosclerosis, fatty liver and maybe neurological disorders [Schebb et al., 2008]. Hence, choline detection is very necessary in clinical analysis, biological sciences, feed additives and food industry. There are various conventional methods have been proposed for the analysis of choline such as high-performance liquid chromatography [Koc et al., 2002; Szilagyi., 1968] and gas chromatography but have many limitations like expensive, complex procedure, experienced operator required time and consuming. Currently, several methods have been developed for the detection of choline based on the enzymatic reaction i.e. choline is react with choline oxidase (ChOx) in the presence of oxygen to produced hydrogen peroxide has been analysed by the optical and electrochemical techniques [Khan et al, 2012]. Still demand to develop a highly stable, inexpensive and simple sensor for detection of choline.

Catalytically active nanomaterials (nanozymes) have explored as an important tool for visual detection with lower cost and better constancy than natural enzymes. Owing to their easy preparation, high stability, good tunability, high catalytic activity, controllable structure, and composition, [Blusztajn, 1998; Schebb et al., 2008] nanozymes have much attention in different applications such as agriculture, drug delivery, nanomedicine, food processing and bio sensing [Su et al., 2015; Zhu et al.,

2015; Lin et al., 2014]. Till now, different type of nanomaterials such as graphene quantum dots [ Nirala et al., 2015; Chen et al., 2017], metal oxides [Liu et al., 2016; Asati et al., 2009], gold nanoparticles [Luo et al., 2010] etc. were showing laccase [ Chiou et al., 2017], oxidase [ Enache et al., 2006], peroxidase [ Liu et al., 2016; Nirala et al., 2015], superoxide dismutase [ Korsvik et al., 2007] and catalase [ Pirmohamed et al., 2010] mimicking activities. Still, quick, sensitive and low cost colorimetric biosensors need to develop based on the robust enzyme mimetic activity.

Due to distinctive physical and chemical properties of new 2D nanomaterials, these are emerging as hot spot areas for researchers. Due the biocompatibility, marvellous catalytic activity and electrical conductivity [Matte et al., 2010; Polyakov et al., 2014] tungsten disulfide ($WS_2$) and Molybdenum disulfide ($MoS_2$) has been increasing research interest along with other 2-D nanomaterials,. Enhanced properties of 2D nanomaterials arises when transformed to zero-dimensional reason being quantum confinement effects and prominent edge [Wang et al., 2016]. In contrast to other nanostructures, $WS_2$-QDs have higher surface area to volume ratio and better electron transport facility.[Anantharaj et al., 2019; Xu et al., 2015] The remarkable properties of $WS_2$-QDs like electronic and optical properties have been applied in the several applications from electronics (FETs and photo detectors etc.) to bio-imaging and biosensors etc.[Singh et al., 2019; Ghorai et al., 2019]

Recently, gold nanoparticles (AuNPs) decorated inorganic semiconductors composite have explored due to enhanced catalytic activity and conductivity for development of highly selective and sensitive biosensors[Su et al., 2014; Blankschien et al., 2013; Chai et al., 2010]. In fact, these materials hold exciting electronic and optical properties which are produced from exciton plasmon coupling and scarce hetero junctions [Tran et

al., 2017]. Other nanocomposites such as carbon derivatives need functionalization for chemical bonding with the gold nanoparticles. [Wang et al., 2012] In contrast, layered transition metal dichalcogenides, like $WS_2$ and $MoS_2$, which contains sulphur atom over the outer layer, are appropriate for metal ligand bond formation of strong Au−S bonds. Due to this chemical bonding, stability of resulting nanocomposites can increase and assist a charge transfer between Au and sulphur. [Sun et al., 2017]

In this work, one-step and simple method proposed for synthesis of AuNPs@$WS_2$-QDs composite. The peroxidase substrate 3, 3', 5, 5'-tetramethylbenzidine (TMB) composite instantly catalyzed by designed material in presence of $H_2O_2$ to produce bluish-green color. Based on the analysis, AuNPs@$WS_2$-QDs composite is applied to detect $H_2O_2$ and choline using colorimetric method. We have proposed a sensing system with an outstanding stability, reproducibility, and selectivity towards choline sensing. Further, the method validated by assay of choline in serum and milk. The designed approach can be used as sensitive colorimetric platform in clinical, pharmaceutical and food inspection field.

## 5.2 Experimental section

### 5.2.1 Chemicals and reagents

30% hydrogen peroxide, sodium tungstatedihydrate ($Na_2WO_4.2H_2O$), L-cysteine, sodium dihydrogen phosphate, disodium hydrogen phosphate and Hydrochloric acid (HCl), were purchased from Merck (Merck, India). Choline oxidase (ChOx), 3, 3', 5, 5'-tetramethylbenzidine (TMB), gold (III) tetrachloride trihydrate ($HAuCl_4.3H_2O$) and horseradish peroxidase (HRP) were bought from sigma Aldrich (USA). Ultrapure water used for the preparation of chemical reagent solutions. Blood samples for analysis of

choline were collected from the authorized hospital, BHU, Varanasi, India. Reagents and Chemicals are used analytical grade without any further purification.

### 5.2.2 Instrumental details

Miniflex 600 X-ray-diffractometer (Cu–Kα radiation, Kα =1.54056 Å, 3°/min scan rate) is used for X-ray diffraction (XRD) measurement in the range between 5° to 80°. UV–vis Epoch 2 microplatereader Biotech (USA) spectrophotometer is used for the absorbance study $WS_2$-QDs and AuNPs@$WS_2$-QD composite in quartz cuvette (1 cm optical path length). Morphological study of materials was done by using HR-TEM, the Energy Dispersive X-ray and EDS mapping by using FEI, TECHNAI $G^2$ 20 TWIN (Czech Republic) electron microscope operating with 200 keV accelerating voltage on a carbon-coated copper grid modified with 6µL solution of the $WS_2$-QDs and AuNPs@$WS_2$-QD composite. Atomic force microscope (AFM) of $WS_2$-QDs and AuNPs@$WS_2$-QDs composite were executed with NT-MDT, Russia on silicon wafer substrate. Zeta potential study of $WS_2$-QDs and AuNPs@$WS_2$-QDs composite were performed through Nanoparticles Analyzer SZ-100, Japan.

### 5.2.3 Experimental procedure for preparation of $WS_2$-QDs

One-step hydrothermal process executed for the synthesis of $WS_2$-QDs. Individual solution of 0.25 g of sodium tungstate and 0.5 g of L-cysteine ($HO_2CCH$ ($NH_2$) $CH_2SH$) and dehydrate ($Na_2WO_4.2H_2O$) were prepared in 25 ml of distilled water (DI) with was were prepared in 25 ml of water with constant stirring for 15 minutes. Then both of the solutions were mixed together followed by continuous stirring at ~40°C and pH (3.0) was maintained by concentrated HCl (12 N). The above mixture solution transferred into Teflon autoclave (100 ml capacity with stainless steel lined) and left for 42 h at

~200°C. After reaction, solution was cooling at room temperature, yellow colloidal solution of $WS_2$-QDs was obtained. The product was dialyzed by dialysis bag (retained molecular weight 2000 Da) for 3-4 days to get the pure $WS_2$-QDs. (Figure 5.1).

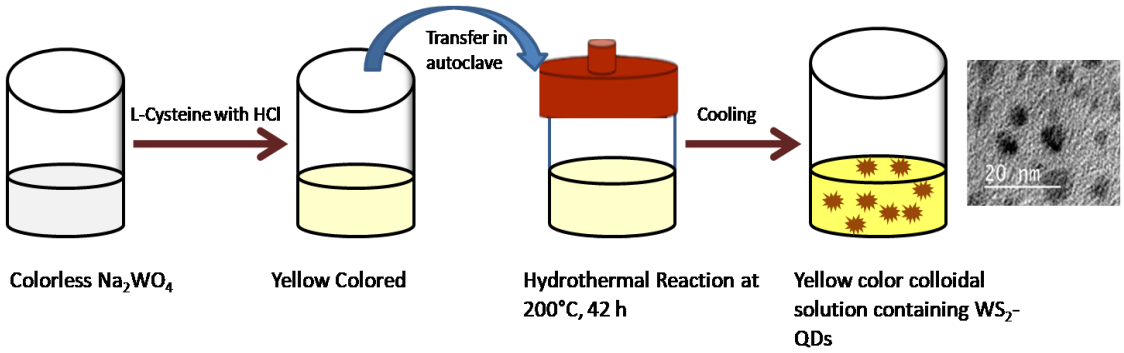


**Figure 5.1** Synthesis of tungsten disulfide-quantum dots ($WS_2$-QDs).

### 5.2.4 Synthesis of AuNPs@$WS_2$-QDs composite

200 µl of prepared $WS_2$-QDs solution was added into 5 ml of aqueous $HAuCl_4$ (1mM) solution at boiling condition with continuous stirring for 30 minutes. The light purple colored solution of AuNPs@$WS_2$-QDs indicates the formation composite system.

### 5.2.5 Choline detection Method

A typical colorimetric method executed for choline detection in buffer: In brief, 20 µL of 2U/mL choline oxidase (ChOx) incubated for 15 min at 40 °C with different choline concentrations (1 to 150 µM) prepared in Phosphate buffer (0.1 M, pH 7.0) for $H_2O_2$ production. Then 20 µL of AuNPs@$WS_2$-QDs composite (1.0 µg/mL) and 30 µL of TMB (2 mM) were added in above solution and pH (4.0) maintained by addition of 200 µL Sodium acetate buffer (0.2 M) incubated 15 min at 40°C to formed TMB oxidation product and absorbance of the reaction solution was recorded at 652 nm.

### 5.2.6 Method for choline detection through test strip in real sample

1.0 M hydrochloric acid used for the extraction of choline from milk samples. Acid digestion liberates bound choline from the milk sample [Pati et al., 2004]. The choline is in free form in serum sample, choline test strip fabricated as AuNPs@$WS_2$-QDs composite system is dip coated in simple cellulose strip and then dried. Further, these strips applied for detection of choline along with proposed color wheel, which rapidly analyse the choline range in serum and milk samples.

## 5.3 Results and discussion

### 5.3.1 Materials characterization

Prepared AuNPs@$WS_2$-QDs composite is flowerlike structure confirmed through TEM images. Also characterized by HR-SEM, XRD, UV-Vis, AFM, zeta, EDS mapping and SAED pattern. UV-Visible spectra of $WS_2$-QDs show absorption maxima at ~248 nm which is characteristic peak of $WS_2$-QDs (Figure 5.2). The result suggests that optical absorption for low dimensional QDs exhibit a strong blue shift when the lateral dimensions reduces to < 50 nm, approved to the quantum confinement. Figure 5.2 (b) represents the enlarged view of AuNPs@$WS_2$-QDs peak in which 600 nm is the characteristic peak of gold nanoparticles.

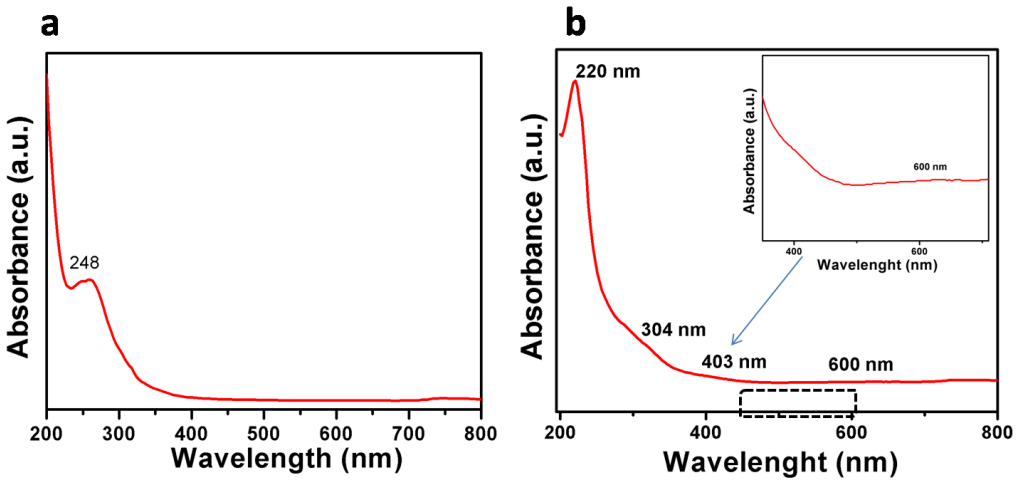


**Figure 5.2** Absorption spectra of (a) $WS_2$-QDs and (b) AuNPs@$WS_2$-QDs, Inset of (b) shows the enlarged view of AuNPs@$WS_2$-QDs peak (600 nm).

The crystal structures of $WS_2$-QDs and AuNPs@$WS_2$-QDs composite executed by XRD measurements in Figure 5.3 (002), (100), (103), (110) faces are assigned to $WS_2$-QDs and the AuNPs@$WS_2$-QDs composite has been assigned (002), (100) due to $WS_2$-QDs and (111), (200), (220), (311) due to gold nanoparticles respectively (CAS no. 84-1398 and 65-2870).

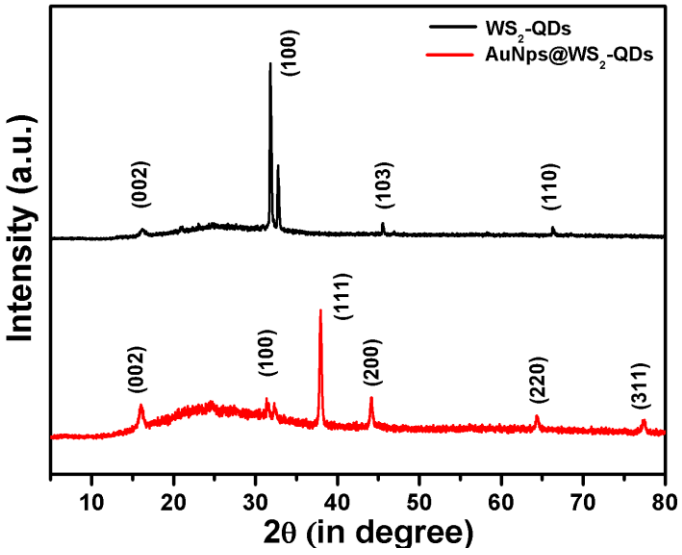


**Figure 5.3** X-ray Diffraction of (a) $WS_2$-QDs (b) AuNPs@$WS_2$-QDs obtained from JCPDS (CAS no. 84-1398 and 65-2870) file.

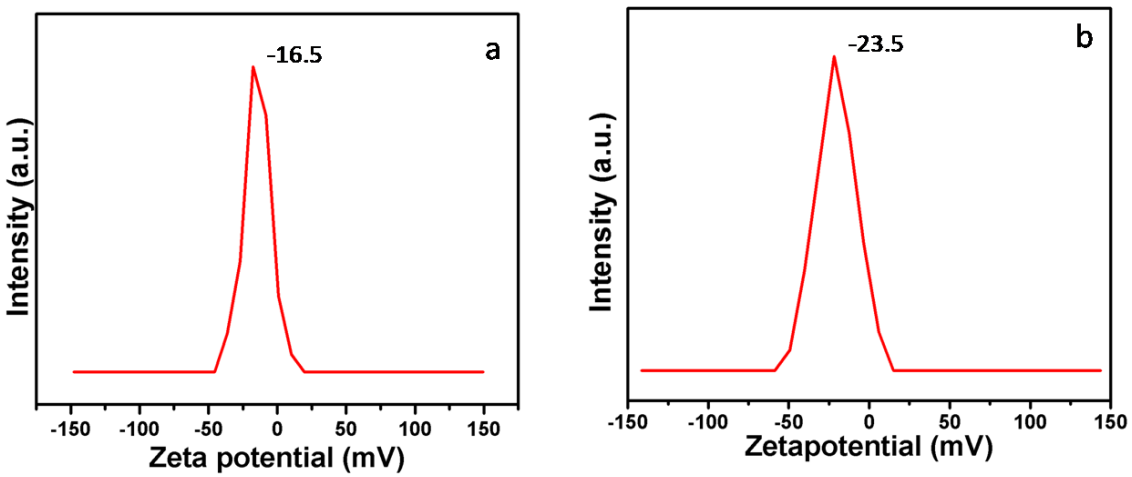


**Figure 5.4** (a) and (b) are the zeta potential graph of $WS_2$-QDs and AuNPs@$WS_2$-QDs respectively.

AuNPs@$WS_2$-QDs composite exhibits strong stability compared to $WS_2$-QDs was investigated by ZETA potential study (-16.5 mV and -23.5 mV for $WS_2$-QDs and AuNPs@$WS_2$-QDs composite respectively) in Figure 5.4 (a and b).

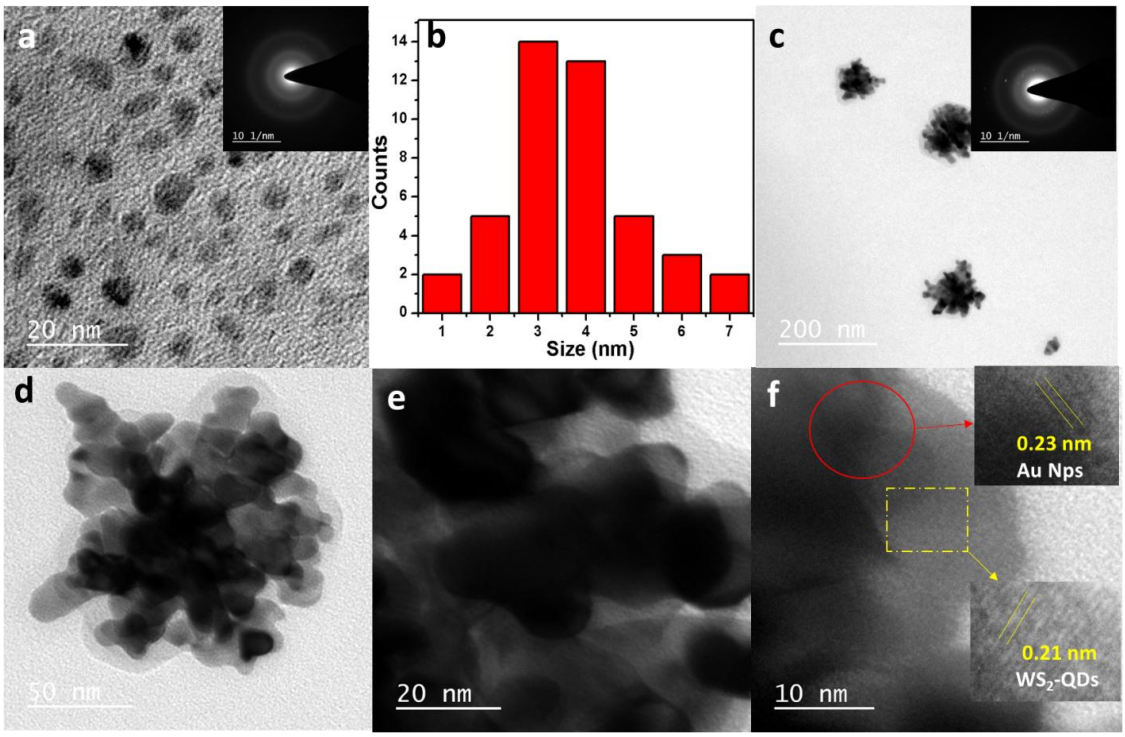


**Figure 5.5** (a) TEM image of $WS_2$-QDs and inset shows SEAD pattern (b) particle size distribution graph of $WS_2$-QDs (c,d,e) TEM image of AuNps@$WS_2$-QDs composite (f) HRTEM image of AuNps@$WS_2$-QDs with lattice fringe spacing of AuNPs ~0.23 nm and $WS_2$-QDs ~0.21 nm and inset of (c) shows SAED pattern of AuNps@$WS_2$-QDs to confirm crystalline nature.

The morphology of prepared nanostructures has revealed by TEM images. Figure 5.5 confirms homogeneous distribution of $WS_2$-QDs with 2-4 nm average size. The inset of Figure 5.5 (a) shows SAED pattern, gives information about crystalline nature $WS_2$-QDs. TEM images of AuNPs@$WS_2$-QDs composite express, $WS_2$-$QD_S$ well decorated over gold nanoparticles to form flower like structure (Figure 5.5c, d, e). The HR-TEM image of AuNPs@$WS_2$-QDs composite(Figure 5.5 f), executes the magnified image of the particular area, inside the yellow box $WS_2$-QDs layers are stacked with lattice fringe spacing ~0.21 nm and under red circle AuNPs have lattice fringe spacing ~0.23 nm, and which is superior with previous existing reports [Gu et al., 2016]. Energy dispersive X-

ray spectroscopy (EDS) mapping of AuNPs@$WS_2$-QDs composite gives information about the elemental composition such as gold, tungsten, sulphur, shown in Figure 5.6.

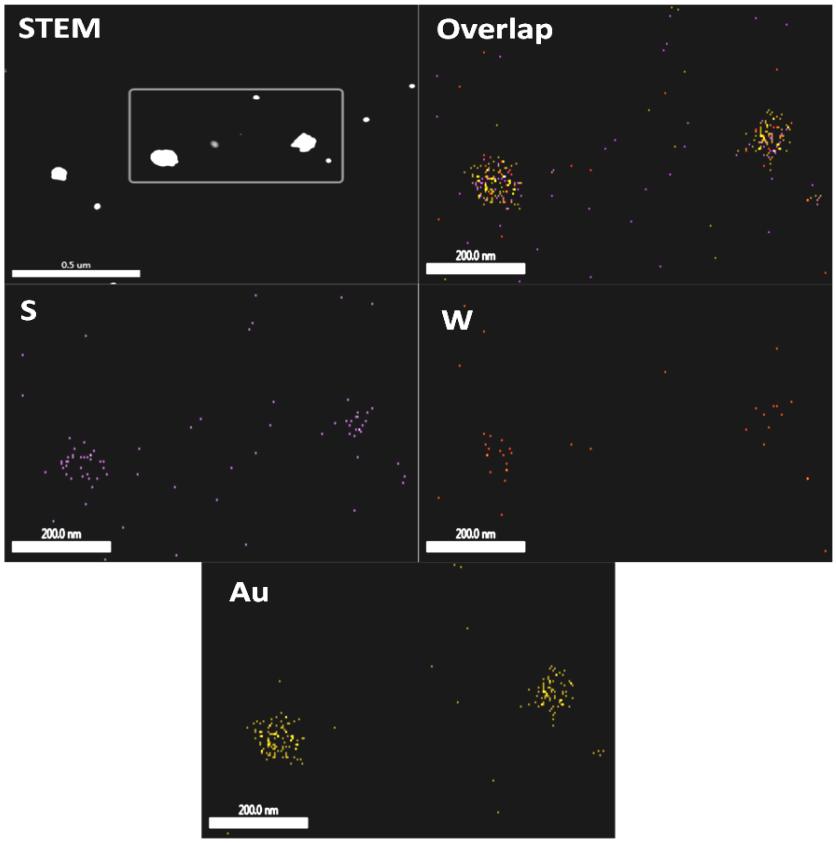


**Figure 5.6** EDS mapping of AuNPs@$WS_2$-QDs composite with overlapped image.

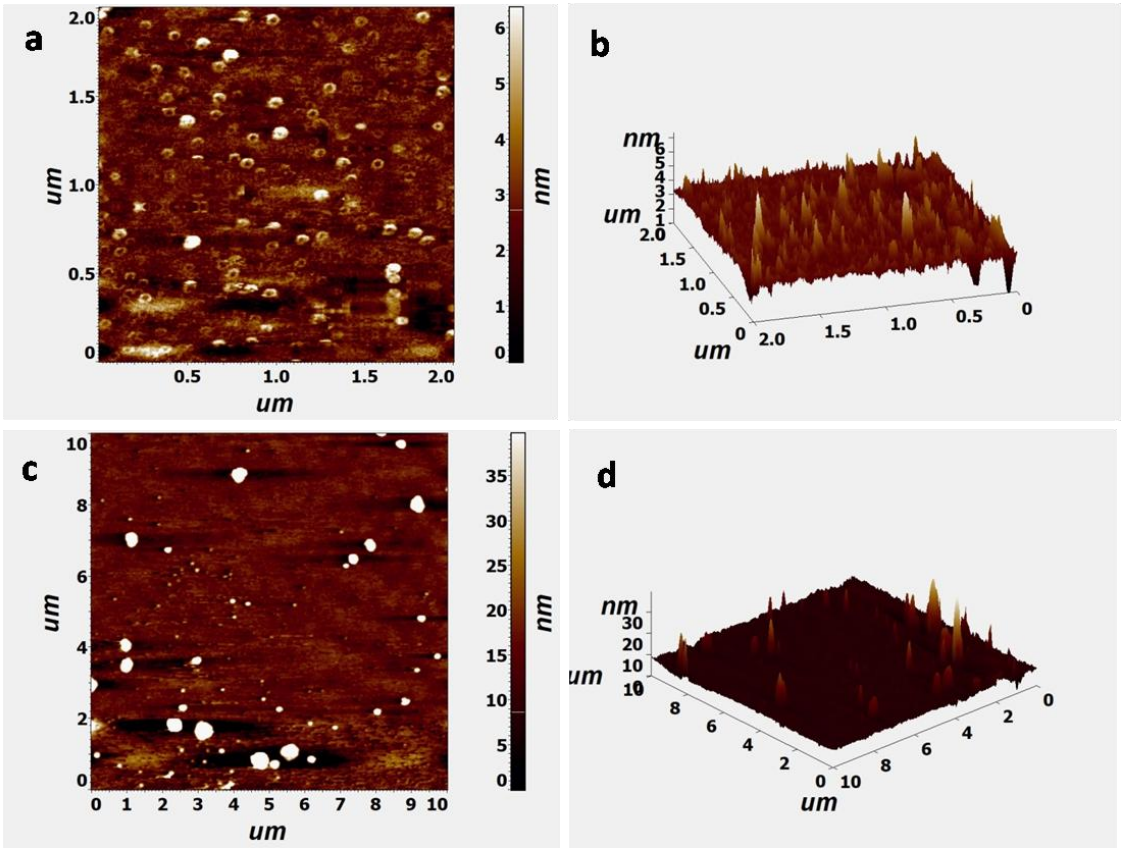


**Figure 5.7** AFM images of $WS_2$-QDs and AuNPs@$WS_2$-QDs composites.

Surface topography of $WS_2$-QD and AuNPs@$WS_2$-QDs composite has been executed by AFM (Figure 5.7). Average thickness is below 6 nm of $WS_2$-QDs and after the composite formation the thickness increases to ~35 nm. of AuNPs@$WS_2$-QDs composites confirms the composite formation.

### 5.3.2 Investigation of enzyme mimetic activity of AuNps@$WS_2$-QDs Composite

Synthesized AuNPs@$WS_2$-QDs composite system has been explored to examine peroxidase like catalytic activity by oxidation of TMB in presence of $H_2O_2$[ Josephy et al., 1982]. The oxidized TMB reveal bluish-green product at 652 nm in the absorbance spectra. Change in the absorbance at 652 nm after addition of $H_2O_2$ and AuNPs@$WS_2$-QDs composite to TMB solution (Figure 5.8a) observed. Typical absorbance peak

intensity at 652 nm with respect to time of AuNPs@$WS_2$-QDs composite-TMB-$H_2O_2$ is high and has faster catalytic activity (Figure 5.8b). Therefore, it indicates that AuNPs@$WS_2$-QDs composite exhibits robust peroxidase mimetic activity towards the TMB substrates.

Possible catalytic mechanism of AuNPs@$WS_2$-QDs composite owing to enhancement of electron transfer leading to increase in mobility and electron density. On AuNPs@$WS_2$-QDs composite surface, TMB substrates are adsorbed and donate lone-pair of electrons of the amino groups to AuNPs@$WS_2$-QDs composite system. After this an increases electron density and mobility of the AuNPs@$WS_2$-QDs composite. Owing to movement of electron density towards the AuNPs@$WS_2$-QDs composite, it confers the participation of the excess electrons in conduction band of AuNPs@$WS_2$-QDs results in a easy electron transfer to the $H_2O_2$, leading to its faster breakdown into hydroxyl and radicals $H_2O$ catalyzed by AuNPs@$WS_2$-QDs composite. The un-oxidized TMB react with hydroxyl radicals and form bluish green color charge transfer complex absorbance maxima at around 652 nm and 350 nm (Figure 5.8a).

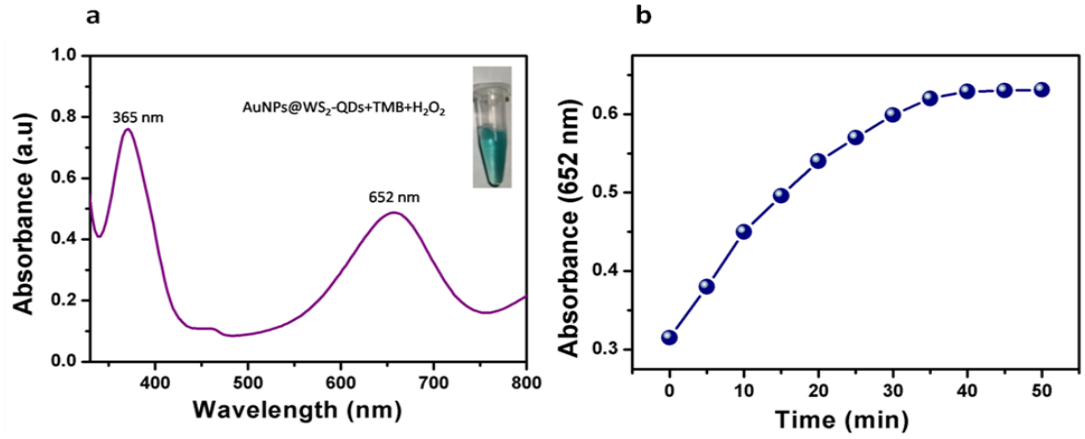


**Figure 5.8** (a) UV-visible absorption spectra of reaction system containing AuNPs@$WS_2$-QDs composite+TMB+$H_2O_2$ (B) Time-dependent absorbance changes at 652 nm of reaction mixture containing AuNPs@$WS_2$-QDs composite, $H_2O_2$, and TMB are 1.0 µg $mL^{-1}$, 0.5 mM, and 2.0 mM respectively.

The mechanism of catalysis of AuNPs@$WS_2$-QDs composite can be explain in the presence of various radical scavengers such as Sodium Azide ($O_2^{\bullet}$ - scavenger), thiourea and ascorbic acid (OH radical scavengers) has been shown in the Figure 5.9. Although, absorbance intensity decreased in the case of thiourea and ascorbic acid as compared to blank sample but there was no change in the absorbance intensity in the case of Sodium Azide, which clearly indicates that, OH radicals are important for the TMB oxidation. Results suggest that for the TMB oxidation, OH radicals are essential.

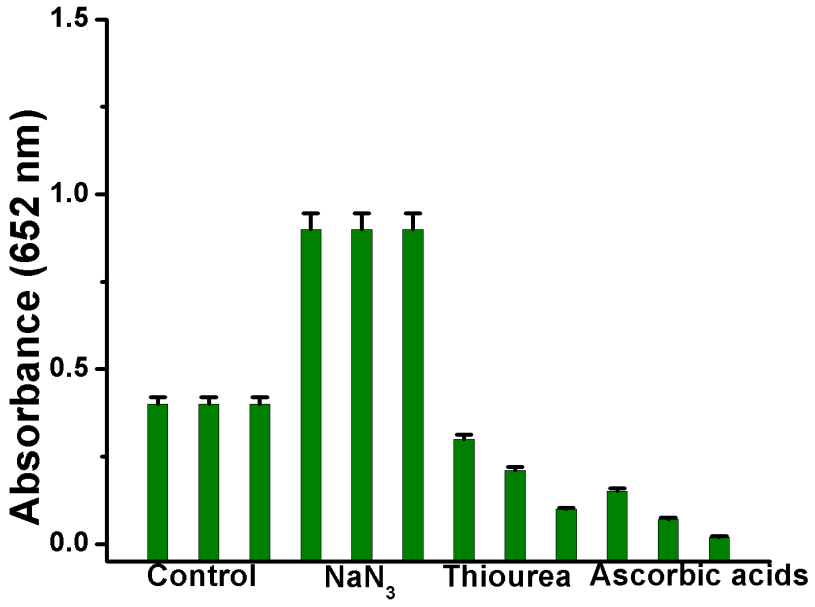


**Figure 5.9** The catalytic reaction system in presence of various radical scavengers.

**Procedures:** 30 µL of AuNPs@$WS_2$-QDs composite (6 µg/mL), 20 µL TMB (1 mM), 50 µL 0.2 M sodium acetate buffer (pH 4.0) and 3 different quantity of radical scavengers were added separately. The volume of solution was making up to 150 µL in water, after that 80 µL of 0.1 mM $H_2O_2$ was added. The reaction was continued for 30 min at the room temperature after that absorbance was recorded at 652 nm. The

concentrations of ascorbic acid, thiourea and $NaN_3$ were taken 1 mM. The error bars stand for the standard error derived from three repeated measurements.

### 5.3.3 Optimizations of methods

Different reaction parameters which are optimized here are reaction time, $H_2O_2$ concentration range, pH value and temperature. The activity of natural enzyme i.e. HRP is mostly affected by the change in pH (lower or higher), temperature (higher) and $H_2O_2$ concentration. AuNPs@$WS_2$-QDs composite shows excellent catalytic activity in the broad range of temperature (25-70 °C) and pH (1.5-10.0) shown in Figure 5.10b, c. The maximum catalytic activity of the AuNPs@$WS_2$-QDs composite be observed at pH 4.0 (acidic medium). The catalytic activity of AuNPs@$WS_2$-QDs composite in broad range of pH would be commercial for the sensing application. AuNPs@$WS_2$-QDs composite system also showed superior catalytic activity in broad range of concentration $H_2O_2$ (Figure 5.10a). Catalytic activity of the AuNPs@$WS_2$-QDs composite is stable at optimum concentration because there are no vacant active sites available at catalyst. The following experimental conditions were established for best result: (a) 20 μL of Choline Oxidase (2 $U \cdot mL^{-1}$); (b) 10 μL of AuNPs@$WS_2$-QDs composite (1 $\mu g \cdot mL^{-1}$); (c) 30 μL of TMB (2 mM); (d) 80 μL of 0.2 M acetate buffer (pH 4.0); (e) incubation time:15 min.; (f) incubation temperature :40 °C.

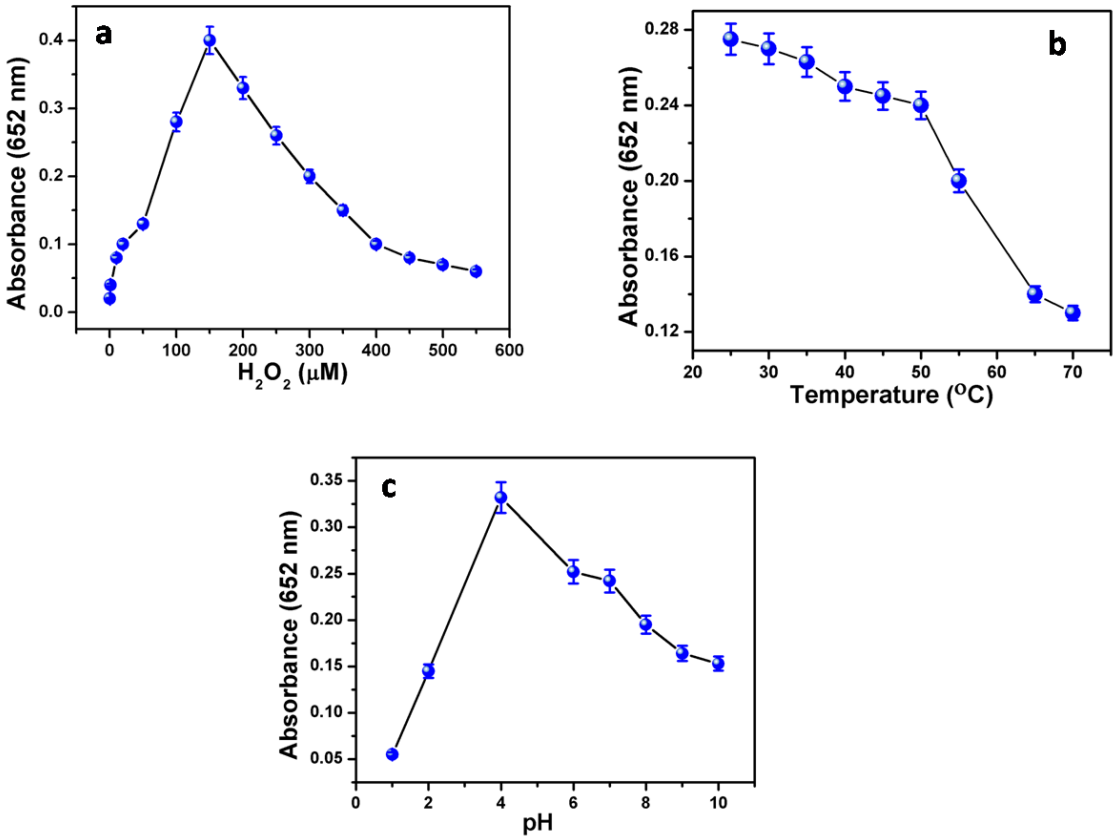


**Figure 5.10** Optimizations of various parameters for catalytic activity of AuNPs@$WS_2$-QDs composite: (a) $H_2O_2$, (b) temperature and (c) pH. Experiments were carried out mixture of AuNPs@$WS_2$-QDs (1 µg.$mL^{-1}$), TMB (1mM) and $H_2O_2$ (0.5 mM) in pH 4.0 maintained by acetate buffer at 40°C.

### 5.3.4 Investigation of Steady state kinetics of AuNPs@$WS_2$-QDs composite

Additional exploration of steady state kinetics of AuNPs@$WS_2$-QDs composite to get perceptible kinetic data chiefly depends on $H_2O_2$ or TMB concentration was varied whereas maintenaning other one concentration constant. Steady state Kinetics of the reaction is calculated *via* Michaelis– Menten equation. The results show that AuNPs@$WS_2$-QDs composite follows Michaelis–Menten behavior for $H_2O_2$ as well as TMB. Lower noticeable Km values for TMB (0.06 mM) and $H_2O_2$ (0.1 mM) of AuNPs@$WS_2$-QDs composite indicates higher affinity towards substrates shows higher catalytic activity of AuNPs@$WS_2$-QDs composite (Figure 5.11). Literature shows that

AuNPs@$WS_2$-QDs composite has superior catalytic activity towards the substrates. Km and Vmax value listed in Table 5.1.

.

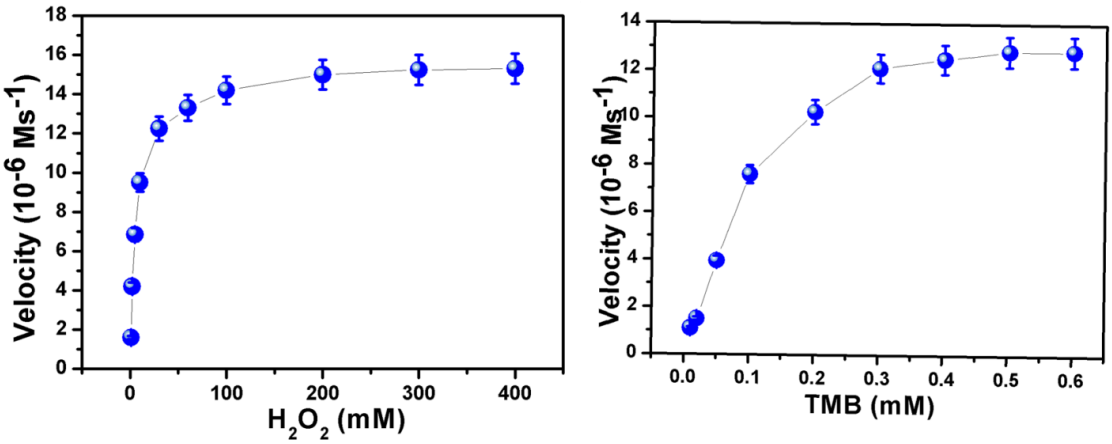


**Figure 5.11** Steady state kinetic measurement of AuNPs@$WS_2$-QDs composite through (a) variation of $H_2O_2$ concentration and fix TMB and (b) variation of TMB concentration and fix $H_2O_2$.

**Table 5.1** Comparative table of steady state kinetics of various catalytic substrates and HRP though TMB oxidation.

| Catalyst | Substance | $K_m$ [mM] | $V_{max}$ [$Ms^{-1}$] | Reference |
|---|---|---|---|---|
| $MoS_2$ | TMB | 0.525 | $5.16\times 10^{-8}$ | Lin et al., 2014 |
| | $H_2O_2$ | 0.0116 | $4.29\times 10^{-8}$ | |
| C-Dots | TMB | 0.039 | $3.61\times 10^{-8}$ | Shi et al., 2011 |
| | $H_2O_2$ | 26.77 | $30.61\times 10^{-8}$ | |
| Si-dots | TMB | 1.502 | $14.72\times 10^{-8}$ | Chen et al., 2014 |
| | $H_2O_2$ | 0.065 | $5.65 \times 10^{-8}$ | |
| HRP | TMB | 0.434 | $10 \times 10^{-8}$ | Chen et al., 2014 |
| | $H_2O_2$ | 3.702 | $8.71 \times 10^{-8}$ | |

| | | | | |
|---|---|---|---|---|
| $MoS_2$ NRs – Au NPs | TMB | 0.015 | $6.7 \times 10^{-6}$ | Nirala et al., 2015 |
| | $H_2O_2$ | 10 | $11.7 \times 10^{-6}$ | |
| AuNPs@$WS_2$-QDs | TMB | 0.06 | $11.8 \times 10^{-6}$ | Present work |
| | $H_2O_2$ | 0.1 | $15 \times 10^{-6}$ | |

### 5.3.5 Colorimetric assay of $H_2O_2$ and choline

Detection of Choline is performed by colorimetric technique based on peroxidase mimetic activity of AuNPs@$WS_2$-QDs composite with TMB in presence of the $H_2O_2$ system. Firstly, different concentrations of $H_2O_2$ were detected in buffer based on TMB oxidation, catalyzed by AuNPs@$WS_2$-QDs composite shown in Figure 5.12 (a).The proposed sensing system performed good linearity from 5 to 200 µM ($R^2$ = 0.99) with a low detection limit, 0.11 µM (Figure 5.12 b). Additionally, color variation for various amount of $H_2O_2$ was visually observed. Colorimetric detection of choline is depends on the concentration of $H_2O_2$ produced from enzymetic reaction of Choline oxidase and choline.

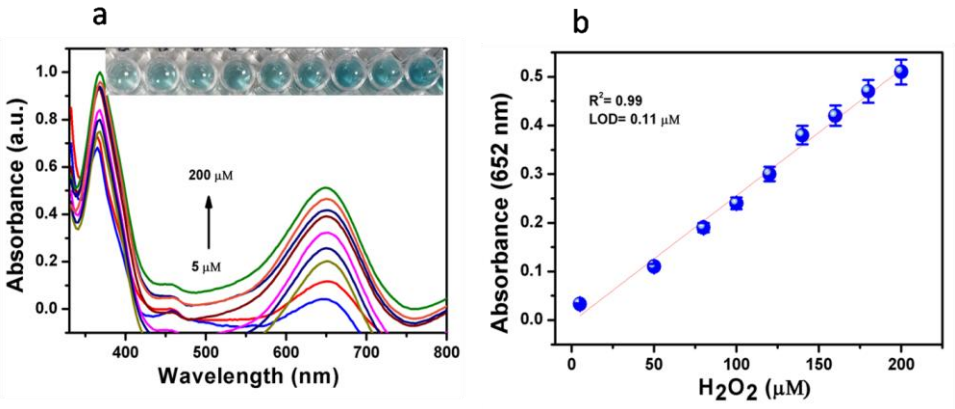


**Figure 5.12 (a)** Concentration dependent UV-Visible graph for $H_2O_2$ detection (1 to 200 µM) and **(b)** linear calibration plot for $H_2O_2$. Inset of **(a)** shows the images of TMB oxidation colored product for different concentration of $H_2O_2$.

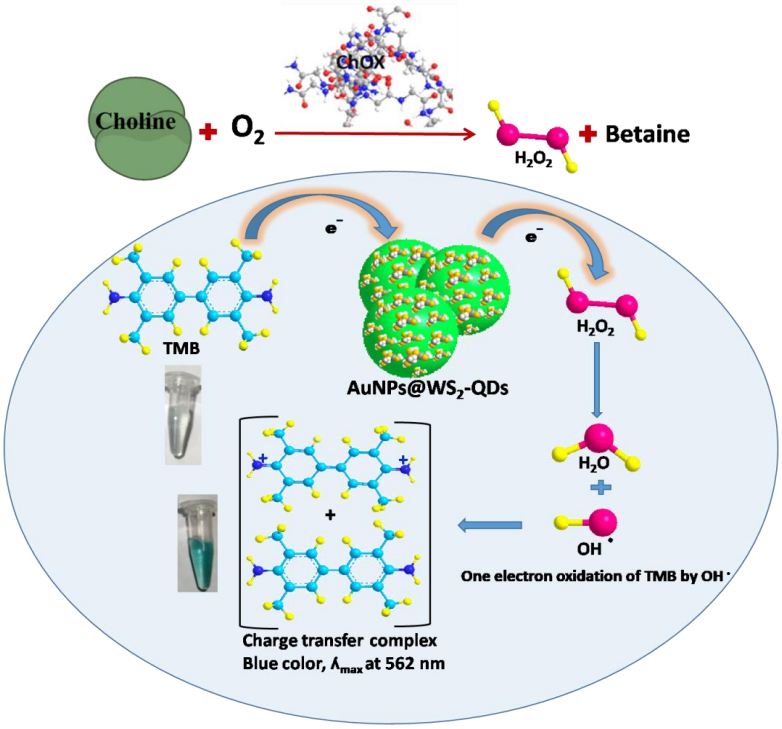


**Figure 5.13** Mechanism of choline detection based on TMB oxidation catalyzed by AuNPs@$WS_2$-QDs composite.

Choline oxidase catalyzes the choline into $H_2O_2$ and betaine in presence of oxygen. Produced $H_2O_2$ utilized in the reaction of TMB oxidation catalyzed by AuNPs@$WS_2$-QDs composite, which produced a blue color reaction product (Figure 5.13). Absorbance intensity varies with various concentration of choline in buffer from dynamic ranges 0 to 150 µM ($R^2$ = 0.997) with a low detection limit i.e. 0.086 µM (Figure 5.14a, b) and color difference was observed from colorless to blue by unaided eye (Inset Figure 5.14a) to measure the choline concentration. In addition, the proposed sensing system has also applied to detect the choline in serum and milk samples (Figure 5.19, 5.18) and obtained result compared with conventional enzymatic methods (Table 5.2).

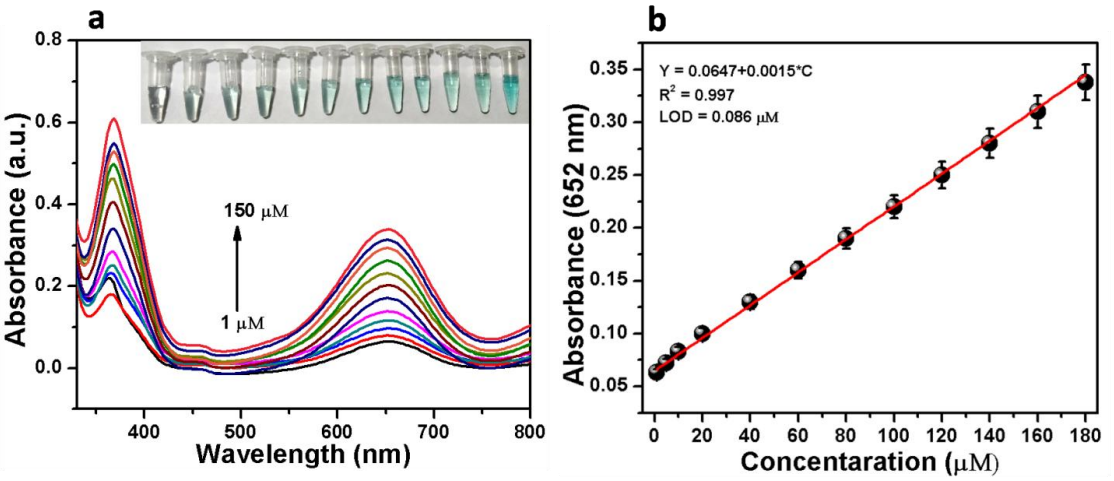


**Figure 5.14** (a) UV-Visible spectra of colorimetric sensing of choline based on AuNPs@$WS_2$-QDs composite + TMB + ChOx in buffer, inset shows visible color of various concentration of choline and (b) corresponding calibration curve at 652 nm.

### 5.3.6 Selectivity and repeatability test

Selectivity test has been studied by using different interference such as 10 mM of ascorbic acid, uric acid, urea, cysteine, cholesterol. The Proposed sensing method is very selective for the choline detection (Figure 5.15 a). Reproducibility test was also performed through the experiment by using six different samples prepared in the same set of conditions shows consistent fine reproducibility (Figure 5.15 b).

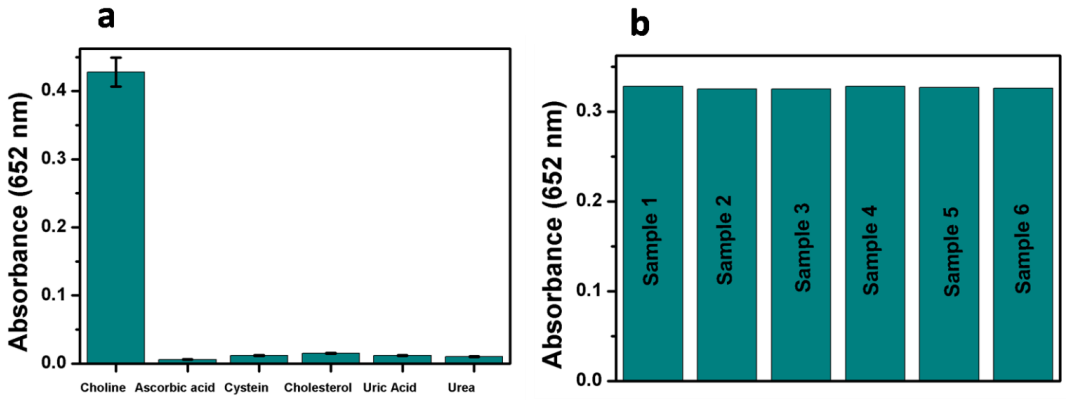


**Figure 5.15** (a) Selectivity analysis AuNPs@$WS_2$-QDs composite system with interfering substances by recording absorbance at 652 nm, including 10.0 mM of ascorbic acid, cysteine, cholesterol, uric acid, urea and (b) reproducibility of six samples prepared in same set of conditions.

### 5.3.7 Production of test strip for choline detection in real sample

In current time, choline detection in the real samples as if serum and milk based on commercial instruments need electrical system and electrical power makes them costly and complex. Here we proposed method for the development of easy and simple dip test strip for visual detection of choline in serum and milk samples by using filter paper as an optical platform (Figure 5.16). The filter paper with negligible background color selected for the detection due to controllable shape and large loading capacity. Firstly, add the mixture of real samples (milk/serum) containing choline into choline oxidase (2 mg/mL) solution and incubated at 4°C for 4 minutes to produce $H_2O_2$ by enzymatic reactions. Then transfer 10 µL of above solution to the slide. Separate dry dip strip with AuNPs@$WS_2$-QDs composite (5µg) and TMB (5 mM) with acetate buffer (pH 4.0) was developed. Finally, dip the test strip in real sample (serum and milk) and observe immediate color change from the colorless to blue due to presence of $H_2O_2$, and then developed color in test strip match with color wheel chart to verify subsequent concentration of the choline present in real sample (Figure 5.17).

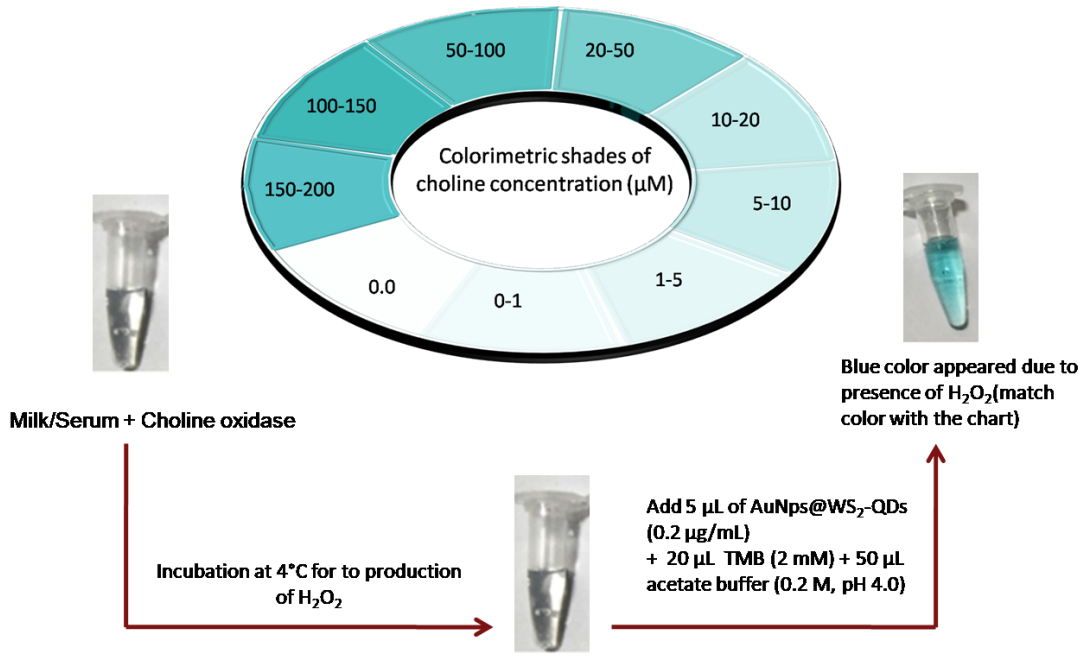


**Figure 5.16** The manufacture of AuNPs@$WS_2$-QDs composite based choline detection test strips for quick detection of choline level by using naked eyes.

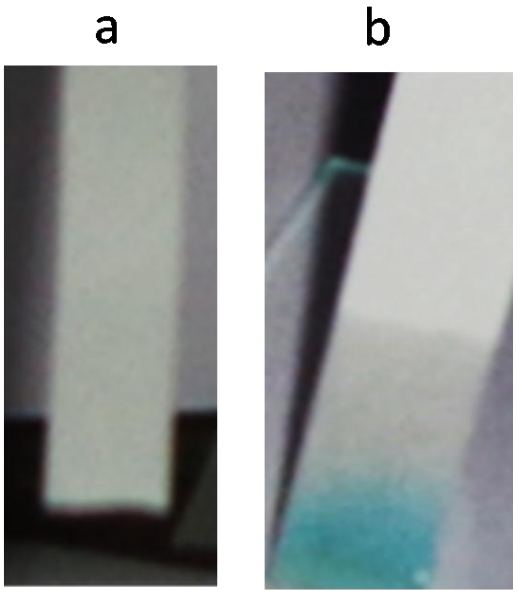


**Figure 5.17** Demonstration of the utility of paper strip in the analysis of choline in real sample. Visualize the choline in real sample by paper strip (a) control,(b) 120 µM.

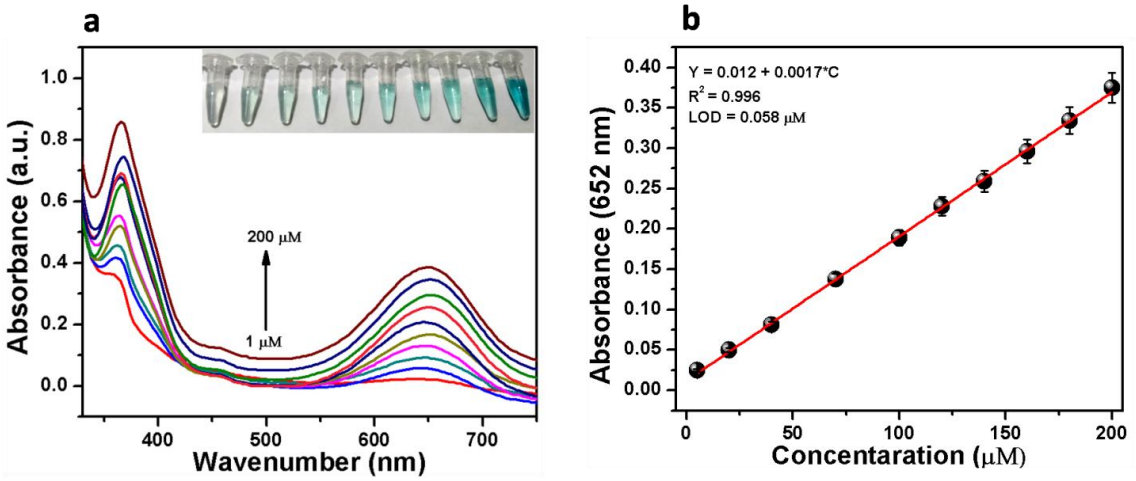


**Figure 5.18.** (a) UV-Visible spectra of colorimetric sensing of choline based on AuNPs@$WS_2$-QDs composite + TMB + ChOx in milk, inset shows visible color of various concentration of choline and (b) corresponding calibration curve at 652 nm.

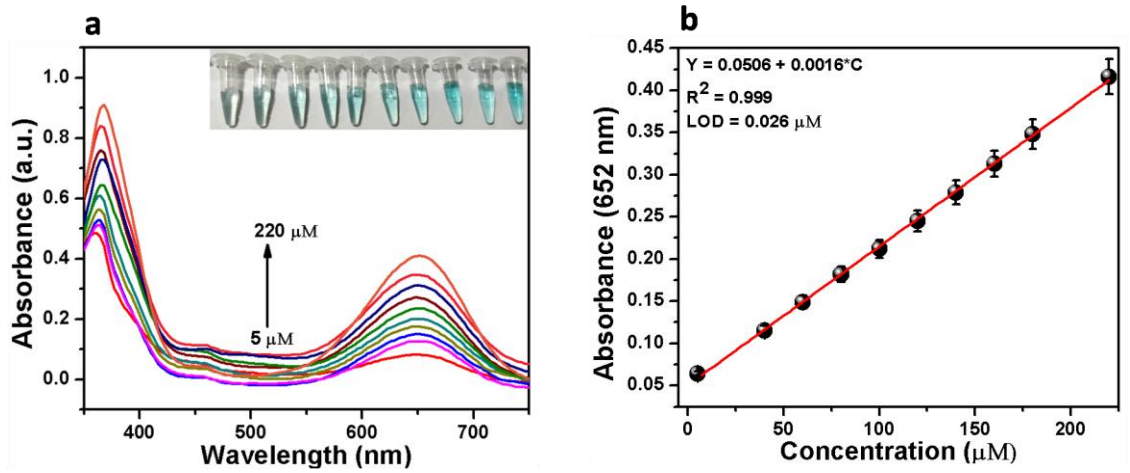


**Figure 5.19** (a) UV-Visible spectra of colorimetric sensing of choline based on AuNPs@$WS_2$-QDs composite + TMB + ChOx in serum, inset shows visible color of various concentration of choline and (b) corresponding calibration curve at 652 nm.

**Table 5.2** The recovery of standard addition of choline in milk.

| S.No. | Added value of choline (μM) | Measured value of choline (μM) | Relative Error (%) |
|---|---|---|---|
| 1 | 20 | 19.8±0.01 | 2±0.01 |
| 2 | 60 | 59.5 ±0.01 | 5±0.01 |
| 3 | 180 | 179.6 ±0.01 | 4±0.01 |

## 5.4 Conclusions

In summary, AuNPs@$WS_2$-QDs composite has been synthesized successfully which shows the peroxidase mimetic activity towards the TMB substrate. TMB was catalyzed by AuNPs@$WS_2$-QDs composite in presence of $H_2O_2$ and formed blue color of the TMB oxidation product, which confirmed peroxidase mimetic activity. The intrinsic peroxidase like catalytic activity of AuNPs@$WS_2$-QDs composite also follows Michaelis-Menten kinetics. The stability and catalytic activity of AuNPs@$WS_2$-QDs composite considerably shows over broad range of pH from 1.5 – 10.0 and temperature 25°C – 70°C. Proposed sensing system is very sensitive and selective towards the colorimetric detection for $H_2O_2$ and choline based on choline oxidase (ChOx) and AuNPs@$WS_2$-QDs composite reaction system. For the development of visual platform, inexpensive, simple paper based test strip was fabricated for detection of the choline in blood serum and milk samples. Additionally the designed scheme has potential to be applied on field and color shade directly compare with amount of choline present in the real samples. Hence, cost effective choline assay strip have been fabricated and Match

with detection color wheel to detect desired choline concentration in the real sample. It is projected that result can support application of the peroxidase mimetic activity of AuNPs@$WS_2$-QDs composite in field of food industry, clinical analysis, biological sciences and other fields.